

Constraining wrong-sign hbb couplings with $h \rightarrow \Upsilon\gamma$ Tanmoy Modak,^{1,*} Jorge C. Romão,^{2,†} Soumya Sadhukhan,^{1,‡} João P. Silva,^{2,§} and Rahul Srivastava^{1,3,||}¹*The Institute of Mathematical Sciences, 600113 Chennai, India*²*CFTP, Departamento de Física, Instituto Superior Técnico, Universidade de Lisboa, Avenida Rovisco Pais 1, 1049 Lisboa, Portugal*³*Physical Research Laboratory, 380009 Ahmedabad, India*

(Received 15 August 2016; published 27 October 2016)

The rare decay $h \rightarrow \Upsilon\gamma$ has a very small rate in the Standard Model, due to a strong cancellation between the direct and indirect diagrams. Models with a changed hbb coupling can thus lead to a great increase in this decay. Current limits on two Higgs doublet models still allow for the possibility that the hbb coupling might have a sign opposite to the Standard Model, the so-called “wrong-sign.” We show how $h \rightarrow \Upsilon\gamma$ can be used to put limits on the wrong-sign solutions.

DOI: 10.1103/PhysRevD.94.075017

I. INTRODUCTION

With the discovery at LHC of the first spin 0 particle [1,2], one must now probe its couplings in detail, searching for discrepancies with the Standard Model (SM) Higgs. Of particular interest is the possibility that the hbb coupling could have a magnitude close to the SM value, but with the opposite sign: the “wrong-sign” solution. Current data are consistent with this possibility [3–5].

There is great interest in the two Higgs doublet model (2HDM) [6,7]. Most attention is devoted to models with a discrete Z_2 symmetry, softly broken by a term with a real coefficient. These models have two charged scalars H^\pm , one pseudoscalar A , a heavy scalar H , and a light scalar h , which we identify as the 125 GeV scalar from LHC. There are four types of such models. Of these, only Type-II and Flipped are consistent with wrong-sign solutions [8–10].

Naturally, a sign change does not affect the $h \rightarrow b\bar{b}$ rate, which, in most models of the 125 GeV scalar, is very close to its total width. Thus, the effect of the wrong-sign must be sought indirectly, for example, through its one-loop contribution to the glue-gluon production $gg \rightarrow h$ and diphoton decay $h \rightarrow \gamma\gamma$. However, there, loops with intermediate bottom quarks compete with much larger contributions from loops with top quarks ($gg \rightarrow h$) or with top quarks and with gauge bosons ($h \rightarrow \gamma\gamma$). As a result, these processes will have values close to the SM, and only a very precise measurement of order 5% in $pp \rightarrow h \rightarrow \gamma\gamma$ will enable experiments to disentangle the normal sign from the wrong-sign solutions [9,11].

In contrast, the rare decay $h \rightarrow \Upsilon\gamma$ involves two diagrams which have almost the same magnitude in the SM.

The decay is very suppressed in the SM (compared, for example, with $h \rightarrow J/\psi\gamma$) due to an accidental cancellation between the two diagrams [12–14]. A change in the hbb sign will destroy the precise cancellation and will have a dramatic effect in this decay [13–15],¹ making $h \rightarrow \Upsilon\gamma$ the prime candidate to probe the wrong-sign solutions. The importance of such a measurement on the wrong-sign solutions of the 2HDM is the subject of this article.

In Sec. II we introduce our notation, and in Sec. III we present the details of the $h \rightarrow \Upsilon\gamma$ decay and perform a full simulation within the real 2HDM. In Sec. IV we draw our conclusions.

II. WRONG-SIGN SOLUTION IN THE 2HDM**A. Notation**

In this article we consider a CP -conserving 2HDM with a discrete Z_2 symmetry, broken softly by a real term, reviewed extensively, for example, in [6,7]. The scalar potential may be written as

$$\begin{aligned}
 V_H = & m_{11}^2 |\Phi_1|^2 + m_{22}^2 |\Phi_2|^2 - m_{12}^2 [\Phi_1^\dagger \Phi_2 + \Phi_2^\dagger \Phi_1] \\
 & + \frac{\lambda_1}{2} |\Phi_1|^4 + \frac{\lambda_2}{2} |\Phi_2|^4 + \lambda_3 |\Phi_1|^2 |\Phi_2|^2 \\
 & + \lambda_4 (\Phi_1^\dagger \Phi_2)(\Phi_2^\dagger \Phi_1) + \frac{\lambda_5}{2} [(\Phi_1^\dagger \Phi_2)^2 + (\Phi_2^\dagger \Phi_1)^2],
 \end{aligned}
 \tag{1}$$

with all coefficients real. The vacuum expectation values are also real and written as $v_1/\sqrt{2}$ and $v_2/\sqrt{2}$. The fields may be parametrized in terms of the mass eigenstates as

*tanmoy@imsc.res.in

†jorge.romao@tecnico.ulisboa.pt

‡soumyasad@imsc.res.in

§jpsilva@cftp.ist.utl.pt

||rahuls@prl.res.in

¹Reference [15] extends the analysis to complex couplings, while Ref. [16] concentrates on the impact in the production mechanism. Exclusive decays into light quarks are also discussed in Ref. [17].

$$\Phi_1 = \begin{pmatrix} c_\beta G^+ - s_\beta H^+ \\ \frac{1}{\sqrt{2}}[vc_\beta + (-s_\alpha h + c_\alpha H) + i(c_\beta G^0 - s_\beta A)] \end{pmatrix},$$

$$\Phi_2 = \begin{pmatrix} s_\beta G^+ + c_\beta H^+ \\ \frac{1}{\sqrt{2}}[vs_\beta + (c_\alpha h + s_\alpha H) + i(s_\beta G^0 + c_\beta A)] \end{pmatrix}, \quad (2)$$

where c_θ (s_θ) is the cosine (sine) of any angle θ in subscript, $\tan \beta = v_2/v_1$, and $v = \sqrt{v_1^2 + v_2^2} = (\sqrt{2}G_F)^{-1/2}$. The fields G^\pm and G^0 are the would-be Goldstone bosons.

We assume that the lightest scalar (h) is the 125 GeV resonance found at LHC. Its couplings with the gauge bosons are

$$\mathcal{L}_{hVV} = \sin(\beta - \alpha)h \left[\frac{m_Z^2}{v} Z^\mu Z_\mu + 2 \frac{m_W^2}{v} W^{+\mu} W_\mu^- \right]. \quad (3)$$

The SM limit corresponds to $\sin(\beta - \alpha) = 1$. We are interested in models with wrong-sign solutions for the fermion couplings. Given current experiments, only Type-II and Flipped are consistent with this possibility [8–10]. In these models, the couplings of h with the fermions from the third family are

$$-\mathcal{L}_{\text{Yuk}} = \frac{m_t}{v} k_U h \bar{t}t + \frac{m_b}{v} k_D h \bar{b}b + \frac{m_\tau}{v} k_\tau h \bar{\tau}\tau, \quad (4)$$

where

$$k_U = \frac{\cos \alpha}{\sin \beta}, \quad k_D = -\frac{\sin \alpha}{\cos \beta}. \quad (5)$$

The only difference between the Type-II and Flipped models lies in the coupling of the charged fermions, given, respectively, by

$$k_\tau = k_D (\text{Type-II}), \quad k_\tau = k_U (\text{Flipped}). \quad (6)$$

The SM limit is $k_U = k_D = k_\tau = 1$.

We will denote the ratios between the 2HDM and SM rates by

$$\mu_f = \frac{\sigma^{2\text{HDM}}(pp \rightarrow h) \Gamma^{2\text{HDM}}[h \rightarrow f] \Gamma^{\text{SM}}[h \rightarrow \text{all}]}{\sigma^{\text{SM}}(pp \rightarrow h) \Gamma^{\text{SM}}[h \rightarrow f] \Gamma^{2\text{HDM}}[h \rightarrow \text{all}]}, \quad (7)$$

where σ is the cross section for Higgs production, $\Gamma[h \rightarrow f]$ is the decay width into the final state f , and $\Gamma[h \rightarrow \text{all}]$ is the total Higgs decay width.

B. A naive explanation for the wrong-sign

For simplicity, let us assume that the production of h is due exclusively to the gluon fusion process with intermediate top quark, and that its width is due exclusively to the decay $h \rightarrow b\bar{b}$. Within these assumptions

$$\sqrt{\mu_{VV}} = \pm \frac{k_U}{k_D} \sin(\beta - \alpha), \quad (8)$$

where the sign (which will be ignored henceforth) is chosen to make the square root positive. Imagine that $\mu_{VV} \sim 1$ because both factors are close to unity. We start by noting that

$$-\frac{k_U}{k_D} = \frac{1}{t_\alpha t_\beta} = \frac{\cos(\beta - \alpha) + \cos(\beta + \alpha)}{\cos(\beta - \alpha) - \cos(\beta + \alpha)}, \quad (9)$$

where t_θ is the tangent of the angle θ . We find that $|k_U/k_D| \sim 1$ if $\beta - \alpha = \pi/2$, in which case $k_D = +1$ (the right-sign solution), or else if $\beta + \alpha = \pi/2$, in which case $k_D = -1$ (the wrong-sign solution).

Now, we look at the second factor in Eq. (8). We find

$$\frac{\sin(\beta - \alpha)}{\sin(\beta + \alpha)} = \frac{1 - \frac{t_\alpha}{t_\beta}}{1 + \frac{t_\alpha}{t_\beta}} = \frac{1 + \frac{1}{t_\beta^2} \frac{k_D}{k_U}}{1 - \frac{1}{t_\beta^2} \frac{k_D}{k_U}}. \quad (10)$$

For $|k_U/k_D| \sim 1$, if t_β is larger than about 3 (say), then

$$\sin(\beta - \alpha) \sim \sin(\beta + \alpha) \left[1 + \frac{2}{t_\beta^2} \frac{k_D}{k_U} \right]. \quad (11)$$

Thus, the second factor in Eq. (8) is very closely given by $\sin(\beta + \alpha)$ already for moderate values of t_β . In conclusion, an experimental constraint of $\mu_{VV} \sim 1$ has a solution $\sin(\beta - \alpha) \sim 1$ for all values of t_β , and it also has a solution $\sin(\beta + \alpha) \sim 1$ for values of $t_\beta \gtrsim 3$. As an illustration, we show in Fig. 1 the constraints on the $\sin \alpha - \tan \beta$ plane of a 20% precision measurement of μ_{VV} around the SM value 1. The left branch corresponds to the right-sign and lies very close to the line $\sin(\beta - \alpha) = 1$ ($k_D = 1$), while the right branch corresponds to the wrong-sign and lies very close to the line $\sin(\beta + \alpha) = 1$ ($k_D = -1$).

We note that, because both factors in Eq. (8) get closer to one in the right-sign and wrong-sign limits, a moderate

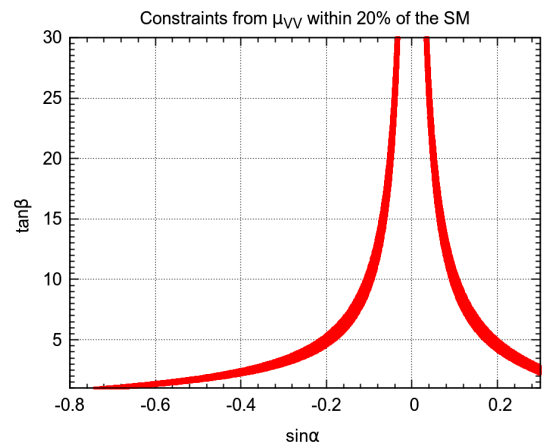


FIG. 1. Constraints from $0.8 \leq \mu_{VV} \leq 1.2$ on the $\sin \alpha - \tan \beta$ plane.

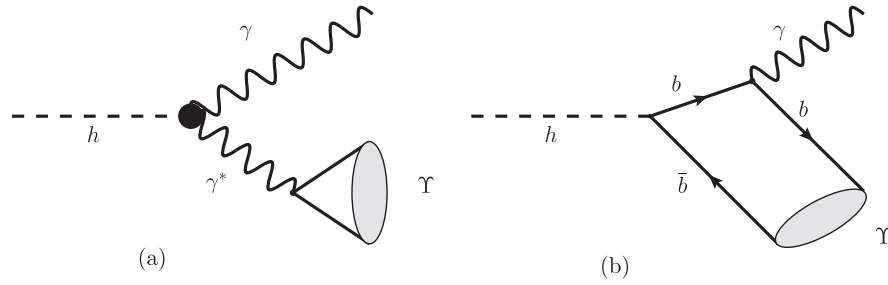


FIG. 2. Feynman diagrams contributing to the $h \rightarrow Y\gamma$ process. The diagrams originate from two different couplings: (a) loop induced $h\gamma\gamma$ (indirect) coupling; (b) $hb\bar{b}$ Yukawa (direct) coupling.

precision in μ_{VV} implies a very precise line in the $\sin\alpha - \tan\beta$ plane [11]. As shown in detail in Sec. II B of [11], for $\tan\beta = 10$ and a precision of 20% in μ_{VV} , $\sin^2(\beta - \alpha)$ is determined to be better than 0.5% in the wrong-sign branch.

III. THE $h \rightarrow Y\gamma$ DECAY IN 2HDM

A. Decay rate

The $h \rightarrow Y\gamma$ decay rate may be written as

$$\Gamma[h \rightarrow Y\gamma] = \frac{1}{8\pi} \frac{m_h^2 - m_Y^2}{m_h^2} |\mathcal{A}_{\text{direct}} + \mathcal{A}_{\text{indirect}}|^2. \quad (12)$$

The direct diagram is shown in Fig. 2(b) and arises from the direct $hb\bar{b}$ coupling (k_D). The indirect diagram is shown in Fig. 2(a) and arises from the effective $h\gamma\gamma$ with a virtual photon morphing into an Y .

We adapt the calculations of Ref. [13] to the 2HDM and write

$$\begin{aligned} \mathcal{A}_{\text{direct}} &= -\eta \frac{2}{\sqrt{3}} e k_D \left(\sqrt{2} G_F \frac{m_Y}{m_h} \right)^{1/2} \\ &\quad \times \frac{m_h^2 - m_Y^2}{m_h^2 - m_Y^2/2 - 2m_b^2} \phi_0(Y), \\ \mathcal{A}_{\text{indirect}} &= \frac{e g_{Y\gamma}}{m_Y^2} (\sqrt{2} G_F)^{1/2} \frac{\alpha m_h^2 - m_Y^2}{\pi} \frac{X}{\sqrt{m_h}} \frac{1}{4}, \end{aligned} \quad (13)$$

where G_F is Fermi's constant, e is the positron charge, k_D is given in Eq. (5), m_Y and m_b are the Y and b -quark masses, α is the fine-structure constant, $\phi_0^2(Y) \sim 0.512 \text{ GeV}^3$ is the wave function of Y at the origin, and

$$g_{Y\gamma} = \frac{2}{\sqrt{3}} \sqrt{m_Y} \phi_0(Y), \quad (14)$$

whose magnitude can be determined from

$$\Gamma[Y \rightarrow \ell^+ \ell^-] = \frac{4\pi\alpha^2(m_Y)}{3m_Y^3} g_{Y\gamma}^2. \quad (15)$$

Our expressions in Eqs. (13) bear three differences with respect to Eqs. (14a) and (14b) of Ref. [13]. First, we have included explicitly in $\mathcal{A}_{\text{direct}}$ the factor $\eta = 0.689$ mentioned at the end of Sec. II A of [13], due to the full next to leading order corrections [13,14]. Second, we have corrected in $\mathcal{A}_{\text{indirect}}$ a $\sqrt{2}$ misprint.² Finally, we have defined $\mathcal{I} = -X/4$, where X is the function arising from the calculation of the effective $h\gamma\gamma$ coupling at one loop in the 2HDM, which can be found in Appendix B of Ref. [18].

As shown in [13], the direct and indirect contributions interfere destructively in an almost complete manner in the SM, and $h \rightarrow Y\gamma$ cannot be detected. This is also the case in the right-sign solution of the 2HDM. In contrast, the wrong-sign solution has a constructive interference, raising the prospects for detection. This is what we turn to next.

B. The importance of $h \rightarrow Y\gamma$ for the wrong-sign scenario

As mentioned, the experimental measurement of μ_{VV} means that the hVV and $h\bar{t}t$ couplings lie close to their SM values. As a result, $h \rightarrow \gamma\gamma$ in the 2HDM is still dominated by the W loop, with a small destructive interference correction from the top loop. There are two novelties in the 2HDM. First, the alteration of k_D . The bottom loop contribution is negligible in the SM. It can indeed change sign in the 2HDM, but, since μ_{VV} places $|k_D| \sim 1$, it cannot have a strong impact. Second, there is a charged Higgs loop. This decouples with the mass of the charged Higgs, but it can still give a contribution of up to 10% for values of the charged Higgs mass around 600 GeV. Such effects are inevitable in the wrong-sign scenario [9]. One concludes that only precise measurements of the $h \rightarrow \gamma\gamma$ decays can yield a signal for the wrong-sign solution of the 2HDM [9,11]; the only method presented thus far.

Here we advocate that $h \rightarrow Y\gamma$ is a good candidate to determine the sign of k_D . This occurs precisely because the cancellation is almost complete in the SM. A change

²We are grateful to G. Bodwin for clarifications on this point. We agree with their Eq. (12), but have a $\sqrt{2}$ difference with respect to their Eq. (14b).

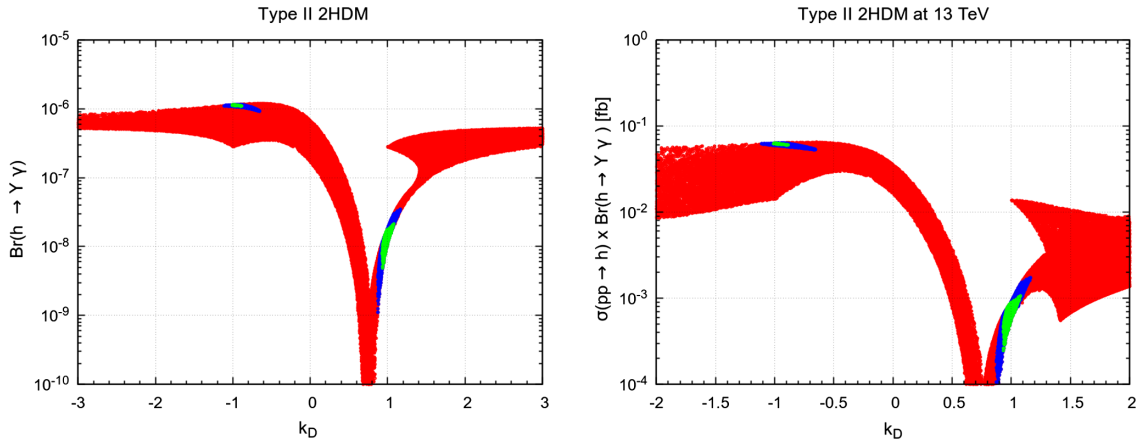


FIG. 3. (a) $\text{BR}(h \rightarrow \Upsilon\gamma)$ as a function of k_D . The red/dark-grey points pass all theoretical constraints in the Type-II 2HDM. The blue/black (green/light-grey) points pass both the theoretical constraints and the experimental constraints on μ_{VV} , $\mu_{\gamma\gamma}$, and $\mu_{\tau\tau}$ at 20% (10%). (b) Same plot, but for $\sigma(pp \rightarrow h) \times \text{BR}(h \rightarrow \Upsilon\gamma)$ at 13 TeV.

in the sign of k_D means that the interference becomes constructive, thus increasing by orders of magnitude the $h \rightarrow \Upsilon\gamma$ decay rate. This can be used to constrain the wrong-sign solution in the 2HDM.

We have performed a full simulation of the real 2HDM, including theoretical constraints from bounded from below potential [19], perturbative unitarity [20–22], oblique radiative parameters [23–25], and we keep $m_{H^\pm} > 480$ GeV to respect B -physics constraints. We include all production mechanisms [26–28] and take μ_{VV} , $\mu_{\gamma\gamma}$, and $\mu_{\tau\tau}$ to lie within 20% of the SM, in close accordance with the latest LHC constraints [29].

The results of our simulation in the Type-II model are shown in Fig. 3. The red/dark-grey points pass all theoretical constraints. The blue/black (green/light-grey) points pass those and also μ_{VV} , $\mu_{\gamma\gamma}$, and $\mu_{\tau\tau}$ at 20% (10%). The situation for the Flipped model is very similar, with only very slight differences in the allowed regions, due to the different dependence on $\mu_{\tau\tau}$.

There are several features of note. After theoretical constraints, the simulation allows for a very large range of k_D . Contrary to what one might naively expect, having a large k_D does not improve much the $h \rightarrow \Upsilon\gamma$ branching ratio. The point is that, although a large k_D does indeed increase the direct amplitude, in accordance with Eq. (13), in the 2HDM the width of h is dominated by $h \rightarrow b\bar{b}$, which also increases with k_D . Once one introduces the experimental constraints, the values for k_D get restricted to right-sign ($k_D \sim 1$) and wrong-sign ($k_D \sim -1$) regions. As explained in Sec. II B, this is mostly due to μ_{VV} and simple trigonometry [11]. Finally, one sees that, due to the same destructive interference at play in the SM, the right-sign solution leads to a minute $h \rightarrow \Upsilon\gamma$ branching ratio around 10^{-8} . In contrast, the wrong-sign solution leads to constructive interference and a $h \rightarrow \Upsilon\gamma$ branching ratio larger by two orders of magnitude.

The possible experimental reach is best seen in Fig. 3(b), where we show a simulation of $\sigma(pp \rightarrow h) \times \text{BR}(h \rightarrow \Upsilon\gamma)$ at 13 TeV. For the wrong-sign, we find a value around 0.06 fb. The current run II data are around 15 fb^{-1} total integrated luminosity [30] and will ultimately achieve around 100 fb^{-1} , meaning that a measurement is becoming possible. This 0.06 fb estimate arises from the precise values taken for $g_{\Upsilon\gamma}$ and the scale chosen for α in the various steps of the calculation. A detailed discussion, including relativistic corrections, can be found in [14]. Our result presents a lower limit on the number of events, meaning that detection prospects are likely to be superior. In fact, using QCD factorization, Ref. [15] finds a SM rate roughly seven times larger than the one quoted in Ref. [14] (illustrating that, given the cancellation between direct and indirect diagrams, precise values do depend on the exact parameter choices). Of course, an even better determination is possible at the High-Luminosity LHC, allowing for the detection or completely ruling out of the wrong-sign solution. We have made a simulation at 14 TeV and obtain the expected increase of about 15% from 0.06 fb into around 0.07 fb, in both Type-II and Flipped.

IV. CONCLUSIONS

The decay $h \rightarrow \Upsilon\gamma$ is very small in the SM, due to a cancellation between the direct and indirect diagrams. In contrast, in theories with a negative hbb coupling, the interference becomes constructive and the rate is increased by orders of magnitude. We have studied this effect on the wrong-sign solution of the Type-II and Flipped 2HDM. We make detailed predictions for the number of events consistent with current bounds on the 2HDM and prove that searches for $h \rightarrow \Upsilon\gamma$ constitute a viable and clean method to constrain the wrong-sign solution, especially at a high luminosity facility.

ACKNOWLEDGMENTS

We are grateful to G. Bodwin for discussions and to R. Santos for carefully reading the manuscript. This work is supported in part by the Portuguese *Fundação para a Ciência e Tecnologia* (FCT) under Contract No. UID/FIS/00777/2013.

-
- [1] G. Aad *et al.* (ATLAS Collaboration), Observation of a new particle in the search for the Standard Model Higgs boson with the ATLAS detector at the LHC, *Phys. Lett. B* **716**, 1 (2012).
- [2] S. Chatrchyan *et al.* (CMS Collaboration), Observation of a new boson at a mass of 125 GeV with the CMS experiment at the LHC, *Phys. Lett. B* **716**, 30 (2012).
- [3] J. R. Espinosa, C. Grojean, M. Muhlleitner, and M. Trott, First glimpses at Higgs' face, *J. High Energy Phys.* **12** (2012) 045.
- [4] A. Falkowski, F. Riva, and A. Urbano, Higgs at last, *J. High Energy Phys.* **11** (2013) 111.
- [5] G. Belanger, B. Dumont, U. Ellwanger, J. F. Gunion, and S. Kraml, Global fit to Higgs signal strengths and couplings and implications for extended Higgs sectors, *Phys. Rev. D* **88**, 075008 (2013).
- [6] J. F. Gunion, H. E. Haber, G. L. Kane, and S. Dawson, *The Higgs Hunter's Guide* (Westview Press, Boulder, CO, 2000).
- [7] G. C. Branco, P. M. Ferreira, L. Lavoura, M. N. Rebelo, M. Sher, and J. P. Silva, Theory and phenomenology of two-Higgs-doublet models, *Phys. Rep.* **516**, 1 (2012).
- [8] A. Celis, V. Ilisie, and A. Pich, Towards a general analysis of LHC data within two-Higgs-doublet models, *J. High Energy Phys.* **12** (2013) 095.
- [9] P. M. Ferreira, J. F. Gunion, H. E. Haber, and R. Santos, Probing wrong-sign Yukawa couplings at the LHC and a future linear collider, *Phys. Rev. D* **89**, 115003 (2014).
- [10] P. M. Ferreira, R. Guedes, M. O. P. Sampaio, and R. Santos, Wrong sign and symmetric limits and non-decoupling in 2HDMs, *J. High Energy Phys.* **12** (2014) 067.
- [11] D. Fontes, J. C. Romão, and J. P. Silva, A reappraisal of the wrong-sign hbb coupling and the study of $h \rightarrow Z\gamma$, *Phys. Rev. D* **90**, 015021 (2014).
- [12] W. Y. Keung, Decay of the Higgs boson into heavy-quarkonium states, *Phys. Rev. D* **27**, 2762 (1983).
- [13] G. T. Bodwin, F. Petriello, S. Stoynev, and M. Velasco, Higgs boson decays to quarkonia and the $H\bar{c}c$ coupling, *Phys. Rev. D* **88**, 053003 (2013).
- [14] G. T. Bodwin, H. S. Chung, J. H. Ee, J. Lee, and F. Petriello, Relativistic corrections to Higgs boson decays to quarkonia, *Phys. Rev. D* **90**, 113010 (2014).
- [15] M. König and M. Neubert, Exclusive Radiative Higgs Decays as Probes of Light-Quark Yukawa Couplings, *J. High Energy Phys.* **08** (2015) 012.
- [16] F. Bishara, U. Haisch, P. F. Monni, and E. Re, Constraining Light-Quark Yukawa Couplings from Higgs Distributions, [arXiv:1606.09253](https://arxiv.org/abs/1606.09253).
- [17] A. L. Kagan, G. Perez, F. Petriello, Y. Soreq, S. Stoynev, and J. Zupan, Exclusive Window onto Higgs Yukawa Couplings, *Phys. Rev. Lett.* **114**, 101802 (2015).
- [18] D. Fontes, J. C. Romão, and J. P. Silva, $h \rightarrow Z\gamma$ in the complex two Higgs doublet model, *J. High Energy Phys.* **12** (2014) 043.
- [19] N. G. Deshpande and E. Ma, Pattern of symmetry breaking with two Higgs doublets, *Phys. Rev. D* **18**, 2574 (1978).
- [20] S. Kanemura, T. Kubota, and E. Takasugi, Lee-Quigg-Thacker bounds for Higgs boson masses in a two doublet model, *Phys. Lett. B* **313**, 155 (1993).
- [21] A. G. Akeroyd, A. Arhrib, and E. M. Naimi, Note on tree level unitarity in the general two Higgs doublet model, *Phys. Lett. B* **490**, 119 (2000).
- [22] I. F. Ginzburg and I. P. Ivanov, Tree level unitarity constraints in the 2HDM with CP violation, [arXiv:hep-ph/0312374](https://arxiv.org/abs/hep-ph/0312374).
- [23] M. E. Peskin and T. Takeuchi, Estimation of oblique electroweak corrections, *Phys. Rev. D* **46**, 381 (1992).
- [24] W. Grimus, L. Lavoura, O. M. Ogreid, and P. Osland, The oblique parameters in multi-Higgs-doublet models, *Nucl. Phys. B* **801**, 81 (2008).
- [25] M. Baak, M. Goebel, J. Haller, A. Hoecker, D. Kennedy, R. Kogler, K. Mönig, M. Schott, and J. Stelzer, The electroweak fit of the standard model after the discovery of a new boson at the LHC, *Eur. Phys. J. C* **72**, 2205 (2012).
- [26] M. Spira, HIGLU: A program for the calculation of the total Higgs production cross section at hadron colliders via gluon fusion including QCD corrections, [arXiv:hep-ph/9510347](https://arxiv.org/abs/hep-ph/9510347).
- [27] R. V. Harlander, S. Liebler, and H. Mantler, SusHi: A program for the calculation of Higgs production in gluon fusion and bottom-quark annihilation in the Standard Model and the MSSM, *Comput. Phys. Commun.* **184**, 1605 (2013).
- [28] LHC Higgs cross section WG picture gallery website, <https://twiki.cern.ch/twiki/bin/view/LHCPhysics/LHCHXSWGCrossSectionsFigures>.
- [29] G. Aad *et al.* (ATLAS and CMS Collaborations), Measurements of the Higgs boson production and decay rates and constraints on its couplings from a combined ATLAS and CMS analysis of the LHC pp collision data at $\sqrt{s} = 7$ and 8 TeV, *J. High Energy Phys.* **08** (2016) 045.
- [30] https://twiki.cern.ch/twiki/bin/view/CMSPublic/LumiPublicResults#Run_2_Annual_Charts_of_Luminosit.